To appear in The Astrophysical Journal

Bardeen-Petterson effect and the disk structure of the Seyfert galaxy NGC 1068

Anderson Caproni and Zulema Abraham

Instituto de Astronomia, Geofísica e Ciências Atmosféricas, Universidade de São Paulo, R. do Matão 1226, Cidade Universitária, CEP 05508-900, São Paulo, SP, Brazil; acaproni@astro.iag.usp.br, zulema@astro.iag.usp.br.

and

Herman J. Mosquera Cuesta [1]

Instituto de Cosmologia, Relatividade e Astrofísica (ICRA-BR), Centro Brasileiro de Pesquisas Físicas, R. Dr. Xavier Sigaud 150, CEP 22290-180, Rio de Janeiro, RJ, Brazil; hermanjc@cbpf.br.

ABSTRACT

VLBA high spatial resolution observations of the disk structure of the active galactic nucleus NGC 1068 has recently revealed that the kinematics and geometry of this AGN is well characterized by an outer disk of H_2O maser emission having a compact milliarcsecond (parsec) scale structure, which is encircling a thin rotating inner disk surrounding a $\sim 10^7$ $M_\odot$ compact mass, likely a black hole. A curious feature in this source is the occurrence of a misalignment between the inner and outer parts of the disk, with the galaxy's radio jet being orthogonal to the inner disk. We interpret this peculiar configuration as due to the Bardeen-Petterson effect, a general relativistic effect that warps an initially inclined (to the black hole equator) viscous disk, and drives the angular momentum vector of its inner part into alignment with the rotating black hole spin. We estimate the time-scale for both angular momenta to get aligned as a function the spin parameter of the Kerr black hole. We also reproduce the shape of the parsec and kiloparsec scale jets, assuming a model in which the jet is precessing with a period and aperture angle that decrease exponentially with time, as expected from the Bardeen-Petterson effect.

[1]Abdus Salam International Centre for Theoretical Physics, Strada Costiera 11, Miramare 34014, Trieste, Italy

Subject headings: galaxies: individual(NGC 1068) — galaxies: active — galaxies: jets — accretion, accretion disks — black hole physics — relativity

1. Introduction

Recent mid-infrared interferometric observations (Jaffe et al. 2004) were able to resolve the inner dust torus of the nearby (14.4 Mpc; Bland-Hawthorn et al. 1997) Seyfert 2 galaxy NGC 1068. The emission distribution along this torus showed a small hot source (probably the accretion disk), surrounded by a parsec-scale warm dust structure.

The hot source coincides with the bright H_2O masers (Greenhill et al. 1996; Gallimore et al. 1996b, 2001, 2004) detected with Very Long Baseline Interferometry (VLBI). The maser emission seems to originate in a sub-Keplerian rotating disk with inner and outer radius corresponding to ∼0.65 and 1.1 pc respectively enclosing, within its inner radius, a black hole and an accretion disk of $\sim 10^7$ $M_\odot$. The departure from Keplerian motion has been attributed to the high mass of the accretion disk that dilutes the gravitational field of the black hole (e.g., Huré 2002; Lodato & Bertin 2003).

The continuum emission at sub-arcsecond scales revealed four components arranged in a jet-counterjet structure, with the core coinciding with the accretion disk position (Wilson & Ulvestad 1987; Muxlow et al. 1996; Gallimore et al. 1996a, 2004). The radio jet orientation changes monotonically with its distance from the core, bending towards the northeast direction. At larger scales, extended lobes are observed, with the northeast lobe having a conic shape, similar to the bow shock structure produced by jet-environment interaction (Wilson & Ulvestad 1987).

An interesting result from maser observations is that the maser disk is not completely aligned with the major axis of the accretion disk across all its extension (e.g., Greenhill & Gwinn 1997; Gallimore et al. 2004). Indeed, they reveal a maser distribution similar to a warped disk, with the inner parts almost perpendicular to the jet, but deviating from this configuration as the distance to the core increases. Gallimore et al. (2004) proposed a configuration in which the thin hot disk is perpendicular to the radio jet, while the misaligned maser disk points towards the parsec-scale dusty-torus.

In this work we investigate the possibility that both the bent jet and warped accretion disk are a consequence of the Bardeen-Petterson effect, which results from the misalignment between the angular momenta of the Kerr black hole and disk. In § 2, we discuss the Bardeen-Petterson mechanism, used to calculate the time-scale for alignment between the two angular momenta. In § 3 we present the physical parameters of the accretion disk of

NGC 1068, as constrained by the observations found in the literature, and we use them to model the warping of the accretion disk due to the Bardeen-Petterson effect as a function of the alignment time-scale. In § 4, we show how jet morphology can be used independently to estimate the alignment time-scale. Conclusions are presented in § 5.

2. The Bardeen-Petterson effect and the alignment time-scale

Frame dragging produced by a Kerr black hole causes precession of a particle if its orbital plane is inclined in relation to the equatorial plane of the black hole. The precession angular velocity $\Omega_{\rm LT}$ due to the Lense-Thirring effect is given by (e.g., Wilkins 1972):

$$\Omega_{\rm LT} = \frac{2G}{c^2}\frac{J_{\rm BH}}{r^3}, \tag{1}$$

where G is the gravitational constant, c is the light speed, r is the radial distance from a black hole of mass $M_{\rm BH}$ and angular momentum $J_{\rm BH}$, defined as $J_{\rm BH} = a_* G M_{\rm BH}^2/c$, with a_* the ratio between the actual angular momentum and its maximum possible value.

The combined action of the Lense-Thirring effect and the internal viscosity of the accretion disk forces the alignment between the angular momenta of the Kerr black hole and the accretion disk. This is known as the Bardeen-Petterson effect (Bardeen & Petterson 1975) and affects only the innermost part of the disk, because of the short range of the Lense-Thirring effect, while its outer parts tend to remain in its original configuration. The transition radius between these two regimes is known as Bardeen-Petterson radius $R_{\rm BP}$, shown schematically in Figure 1; its exact location depends mainly on the physical properties of the accretion disk (Bardeen & Petterson 1975; Kumar & Pringle 1985; Ivanov & Illarianov 1997; Nelson & Papaloizou 2000; Lubow, Ogilvie & Pringle 2002; Fragile & Anninos 2005).

The time-scale for alignment can be calculated as (e.g., Natarajan & Armitage 1999):

$$T_{\rm align} = J_{\rm BH}\left(\frac{dJ_{\rm BH}}{dt}\right)^{-1}\sin\varphi, \tag{2}$$

where φ is the angle between the black hole spin axis and the direction perpendicular to the outer disk. The time derivative of $J_{\rm BH}$ has the form:

$$\frac{dJ_{\rm BH}}{dt} = -2\pi\sin\varphi\int_{R_{\rm BP}}^{R_{\rm out}}\Omega_{\rm LT}(r)L_{\rm d}(r)r\,dr, \tag{3}$$

where $R_{\rm out}$ is the outer disk radius and $L_{\rm d}(r) = \Sigma_{\rm d}(r)\Omega_{\rm d}(r)r^2$ is its differential angular momentum (e.g., Caproni, Mosquera Cuesta & Abraham 2004). $\Omega_{\rm d}$ is the disk angular velocity and $\Sigma_{\rm d}$ is the surface density of the accretion disk integrated over its semi-thickness $H_{\rm d}$, derived following Sakimoto & Coroniti (1981) (see also Bardou, Heyvaerts & Duschl 1998):

$$H_{\rm d}(r) = \frac{H_{\rm nsg}(r)H_{\rm sg}(r)}{\sqrt{H_{\rm nsg}^2(r) + H_{\rm sg}^2(r)}} \tag{4}$$

where $H_{\rm nsg} = c_{\rm s}/\Omega_{\rm d}$, $H_{\rm sg} = c_{\rm s}^2/(\pi G\Sigma_{\rm d})$ and $c_{\rm s}$ is the sound speed, defined as:

$$c_{\rm s}(r) = \sqrt{-\Gamma\frac{d\ln\Omega_{\rm d}(r)}{d\ln r}\frac{\nu_1(r)\Omega_{\rm d}(r)}{\alpha}}, \tag{5}$$

where Γ is the politropic index of the gas, which we have assumed equal to 5/3.

A rough estimate of $R_{\rm BP}$ can be obtained comparing the time-scales for Lense-Thirring precession and warp transmission through the disk (e.g., Natarajan & Armitage 1999) that, on the other hand, will depend on how the warps are being communicated along it. If they are transmitted diffusively:

$$R_{\rm BP}^{\rm diff} = \sqrt{\nu_2/\Omega_{\rm LT}}, \tag{6}$$

where ν_2 is the viscosity acting on the direction perpendicular to the disk; both parameters must be calculated at $R_{\rm BP}^{\rm diff}$. If the time-scales for the warp and surface density evolution are similar $\nu_2 \sim \nu_1$, where ν_1 is the viscosity along the disk; otherwise $\nu_2 \sim f(\alpha)\nu_1$, where $f(\alpha)$ is a function of the dimensionless viscosity parameter α introduced by Shakura & Sunyaev (1973); we adopted $f(\alpha) = 2(1+7\alpha^2)/[\alpha(4+\alpha^2)]$ as derived by Ogilvie (1999). Assuming that the inner radius of the accretion disk is the marginally stable orbit $R_{\rm ms}$, the viscosity ν_1 can be written as:

$$\nu_1 = -\frac{\dot{M}}{2\pi\Sigma_{\rm d}(r)}\left[\frac{d\ln\Omega_{\rm d}(r)}{d\ln r}\right]^{-1}\left[1-\left(\frac{R_{\rm ms}}{r}\right)^2\frac{\Omega_{\rm d}(R_{\rm ms})}{\Omega_{\rm d}(r)}\right], \tag{7}$$

$\dot{M}$ is the accretion rate, which is related to the bolometric luminosity $L_{\rm bol}$ through $\dot{M}/\dot{M}_{\rm Edd} = L_{\rm bol}/L_{\rm Edd}$, where $\dot{M}_{\rm Edd}$ and $L_{\rm Edd}$ are the Eddington mass accretion rate and luminosity, respectively.

In the wave-like regime:

$$R_{\rm BP}^{\rm w} = c_{\rm s}/\Omega_{\rm LT}. \tag{8}$$

The transition from the diffusive to wave-like regime occurs at a radius $R_{\rm T} \sim H_{\rm d}/\alpha$ (Papaloizou & Lin 1995).

3. Application to the accretion disk of NGC 1068

The physical parameters of the black hole accretion disk system of NGC 1068 were determined by Huré (2002) and Lodato & Bertin (2003) from the analysis of the maser line velocities; they are presented in Table 1 and were used in our calculations of the Bardeen-Petterson radius and the alignment time-scale.

The maser velocities present signatures of sub-Keplerian motion; however, in equation (3) we used the relativistic Keplerian angular velocity (Abramowicz, Jaroszyński & Sikora 1978), since at the radius in which this assumption is not valid, the angular momentum $L_{\rm d}$ becomes negligible.

We assumed a power-law surface density distribution for the accretion disk $\Sigma(r) = \Sigma_0(r/R_{\rm g})^s$, where $R_{\rm g} = GM_{\rm BH}/c^2$ is the gravitational radius and $s = -1.05$ (Huré 2002). The constant Σ_0 was determined from the mass of the disk $M_{\rm d}$, derived by Huré (2002) and Lodato & Bertin (2003), integrating $\Sigma(r)$ from the inner to the outer disk radius.

The α-parameter was obtained from the expression $\dot{M} = (28.1 \pm 0.2)\alpha$ M$_\odot$ yr^{-1} given by Lodato & Bertin (2003). The accretion rate can be calculated from the bolometric luminosity $L_{\rm bol} = \epsilon \dot{M} c^2$, given the accretion efficiency ϵ, which depends on the black hole spin parameter a_*. We used as lower limit for the bolometric luminosity $\sim 7 \times 10^{44}$ erg s^{-1}, as found by Gallimore et al. (2004) from the observed free-free emission, and the Eddington luminosity $L_{\rm Edd}$ as upper limit.

The Bardeen-Petterson radius was obtained from either equation (6) or (8), depending if it obeys the diffusive or wave regimes, respectively.

The calculations were performed for the disk models A and B defined in Table 1, considering several values of the black hole spin and the extreme values of the accretion rate and α parameter, the latter depending also on the spin value. The results show that the Bardeen-Petterson radius for NGC 1068 depends weakly on the accretion rate, being limited by the variation of the black hole spin and α parameters between 10^{-5} and 10^{-4} pc (about

20 and 200 Rg respectively) as shown in left panel of Figure 2.

For the lower limit of the α parameter and both black hole masses, $R_{\rm BP} = R_{\rm BP}^{\rm w}$ when $|a_*| > 0.1$. For the upper limit of α, $R_{\rm BP} = R_{\rm BP}^{\rm diff}$ for $a_* < 0.1$, turning gradually into $R_{\rm BP}^{\rm w}$ for larger values of a_* at a rate that depends on the α parameter.

We calculated the alignment time-scale as a function of the black hole spin by solving the integral given in equation (3), using as integration limits the Bardeen-Petterson radius and an arbitrary outer radius. The results, which are independent of the outer radius value, are presented in the right panel of the Figure 2.

The alignment time-scale turned out to vary between 100 and 10^5 yr, while the lifetime of the radio jet in NGC 1068 is $\lesssim 1.5 \times 10^5$ yr (Capetti et al. 1999), similar to the lifetimes of AGN activity. Therefore, it indicates that the Bardeen-Petterson effect can perfectly warp the inner part of the accretion disk.

It is important to emphasize that warped accretion disks produced by the Bardeen-Petterson effect can be probed by features in relativistically broadened emission iron-line profiles (Fragile, Miller & Vandernoot 2005) but unfortunately, since NGC 1068 is a type 2 Seyfert galaxy, relativistically broadened iron-lines are unlikely to be observed due to the obscuring dust torus.

4. Probing alignment from jet kinematics

The current angular resolution provided by interferometric techniques is not capable to resolve structures with sizes comparable to the Bardeen-Petterson radius in NGC 1068. However, the orientation of the inner part of the disk can be traced from the jet, which is usually thought (sometimes supported by observations; Ray et al. 1996; Jones et al. 2000) to be ejected in the perpendicular direction. In NGC 1068, the jet is not continuous but presents discrete features, the upper limit to their expanding velocities being $0.17c$ (Gallimore, Baum & O'Dea 1996).

The Bardeen-Petterson effect forces the disk to align gradually with the black hole, producing precession and a progressive change in the jet direction (Caproni, Mosquera Cuesta & Abraham 2004). According to Scheuer & Feiler (1996), the solution of equation (3) gives an exponential time variation for the inclination angle between black hole spin and the jet direction, as well as for the precession period $P_{\rm prec}$:

$$\varphi(t) = \varphi_0 e^{-(t-t_0)/T_{\rm align}} \tag{9}$$

$$P_{\rm prec}(t) = P_0 e^{-(t-t_0)/T_{\rm align}} \tag{10}$$

where φ_0 and P_0 are, respectively, the inclination angle and precession period at time t_0 when the disk was formed ($t_0 \leq 0$, measured in the past from the present time). Scheuer & Feiler (1996) found that the timescales for precession and realignment are identical, implying that $P_0 = T_{\rm align}$, which will be also consider in our approach.

We assumed that the jet originated at time t_0, afterwards each plasma element was ejected with constant speed $v_{\rm jet}$ at a time t, in a direction that forms an angle $\varphi(t)$ with the black hole spin axis, in a plane that rotates with velocity $\omega(t) = 2\pi/P_{\rm prec}(t)$. We introduced two additional parameters: the viewing and position angle of the black hole spin in relation to the line of sight θ and on the plane of the sky η.

In order to compare our model with the observations, we calculated the right ascension and declination offsets ($\Delta\alpha$ and $\Delta\delta$ respectively) of each jet element as a function of time through:

$$\Delta\alpha(t) = \frac{v_{\rm jet} t}{D} \left[A(t)\cos\eta + B(t)\sin\eta\right], \tag{11}$$

$$\Delta\delta(t) = \frac{v_{\rm jet} t}{D} \left[-A(t)\sin\eta + B(t)\cos\eta\right], \tag{12}$$

where D is the distance to the observer, $A(t) = \sin\varphi(t)\cos\omega t$ and $B(t) = \sin\varphi(t)\sin\omega t\cos\theta + \cos\varphi(t)\sin\theta$.

We found solutions for several combinations of the input parameters, in the range $25^\circ \lesssim \varphi_0 \lesssim 45^\circ$, $70^\circ \lesssim \theta \lesssim 90^\circ$ and $14^\circ \lesssim \eta \lesssim 20^\circ$. The parameters t_0 and $T_{\rm align}$ are scaled by the jet velocity, ranging between $-1.7\times10^5 \lesssim t_0$ (yr)$\lesssim -9600$ and $7500 \lesssim T_{\rm align}$ (yr)$\lesssim 1.3\times10^5$ for $0.01c \lesssim v_{\rm jet} \lesssim 0.17c$ (Wilson & Ulvestad 1987; Gallimore, Baum & O'Dea 1996). The limits found for $T_{\rm align}$ are perfectly compatible with those derived in last section.

In Figure 3 we present the comparison between the parsec and kiloparsec scale radio maps (Wilson & Ulvestad 1987; Gallimore et al. 2004) and a model with parameters $\theta = 80^\circ$, $v_{\rm jet} = 0.17c$, $t_0 = -9800$ yr, $T_{\rm align} = 7580$ yr, $\varphi_0 = 40^\circ$ and $\eta = 17^\circ$. We can see that our simple kinematic approach reproduces satisfactorily the inverted S-shape of the kiloparsec jet, as well as the location of its jet components; at parsec-scales, the position of the jet components C and NE, as well as the counterjet knot S2 are also well-reproduced by the same model. As it can be seen in the left panel of Figure 3, at larger distances from the

core, the full range of position angles provided by our precessing model is not found in the observational data, in the sense that the amplitude of the helix towards the northern and southern regions are systematically larger than the observed jet aperture. This may be due to the implicit assumption of accretion disk rigid-body precession during all the jet-time evolution, which might not be totally true, specially close to the initial time t_0. In fact, numerical simulations have shown a period of differential precession preceding the rigid-body configuration (Nelson & Papaloizou 2000; Fragile & Anninos 2005). In addition, the galactic medium will influence the jet propagation, as can be seen from the [O III] and mid-infrared images of NGC 1068 (Gallimore et al. 1996a; Capetti, Axon & Macchetto 1997; Galliano et al. 2003), showing the existence of jet-ambient interaction.

In all cases considered in this work, the inner disk is not completely aligned with the equator of the black hole since $\varphi \sim 11^\circ$ at the present time. Interestingly, Galliano et al. (2003) proposed the existence of a slight tilt of $\sim 15^\circ$ between the Compton thick central absorber and the molecular disc in order to reproduce the observed distribution of H_2 and CO emission in this object.

5. Conclusions

We studied the possibility that the Bardeen-Petterson effect is responsible for the warping of the accretion disk in NGC 1068, as derived from the radio continuum and water maser observations (e.g., Greenhill & Gwinn 1997; Gallimore et al. 2004). Such mechanism arises from the frame dragging produced by a Kerr black hole whose rotation axis is not parallel to that of the accretion disk.

Using an analytical approach, similar to that suggested by Scheuer & Feiler (1996) and Natarajan & Armitage (1999), we calculated the Bardeen-Petterson radius and the alignment time-scale between the accretion disk and the equator plane of the black hole for different values of the black hole spin. We found that the Bardeen-Petterson radius is roughly limited between 10^{-5} and 10^{-4} pc, while the alignment time-scale ranges from about 100 to 10^5 yr. Those estimates are perfectly compatible with the upper limit to the AGN lifetime, derived from the jet kinematics.

We also showed that the general form of the parsec and kiloparsec scale jets can be reproduced by the model in which the jet is precessing with a period $P_{\rm prec}$ and aperture angle φ that decrease exponentially with a time-scale $T_{\rm align}$, as expected from the Bardeen-Petterson effect.

This work was supported by the Brazilian Agencies FAPESP and CNPq. We thank the anonymous referee for her/his useful comments.

REFERENCES

Abramowicz, M., Jaroszyński, M., & Sikora, M. 1978, A&A, 63, 221

Bardeen, J. M. & Petterson, J. A. 1975, ApJ, 195, L65

Bardou, A., Heyvaerts, J., & Duschl, W. 1998, A&A, 337, 966

Bland-Hawthorn, J., Gallimore, J. F., Tacconi, L. J., Brinks, E., Baum, S. A., Antonucci, R. R. J., & Cecil, G. N. 1997, Ap&SS, 248, 9

Capetti A., Axon D. J., Macchetto F. D. 1997, ApJ, 487, 560

Capetti A., Axon D. J., Macchetto F. D., Marconi A., Winge C., 1999, ApJ, 516, 187

Caproni, A., Mosquera Cuesta, H. J. & Abraham, Z. 2004, ApJ, 616, L99

Fragile, P. C. & Anninos, P., 2005, ApJ, 623, 347

Fragile, P. C., Miller, W. A., & Vandernoot, E. 2005, astro-ph/0507309

Galliano E., Alloin D., Granato G. L., Villar-Martýn M., 2003, A&A, 412, 615

Gallimore, J. F., Baum, S. A., O'Dea, C. P., & Pedlar, A. 1996a, ApJ, 458, 136

Gallimore, J. F., Baum, S. A., O'Dea, C. P., Brinks, E., & Pedlar, A. 1996b, ApJ, 462, 740

Gallimore, J. F., Baum, S. A., & O'Dea, C. P. 1996, ApJ, 464, 198

Gallimore, J. F., Henkel, C., Baum, S. A., Glass, I. S., Claussen, M. J., Prieto, M. A., & Von Kap-herr, A. 2001, ApJ, 556, 694

Gallimore, J. F., Baum, S. A., & O'Dea, C. P., 2004, ApJ, 613, 794

Greenhill, L. J., Gwinn, C. R., Antonucci, R., & Barvainis, R. 1996, ApJ, 472, L21

Greenhill, L. J., & Gwinn, C. R. 1997, Ap&SS, 248, 261

Huré, J.-M. 2002, A&A, 395, L21

Ivanov, P. B., Illarianov, A. F. 1997, MNRAS, 285, 394.

Jaffe, W., et al. 2004, Nature, 429, 47

Jones, D. L., Wehrle, A. E., Meier, D. L., Piner, B. G. 2000, ApJ, 534, 165

Kumar, S., Pringle, J. E. 1985, MNRAS, 213, 435.

Lodato, G., & Bertin, G. 2003, A&A, 398, 517

Lubow, S. H., Ogilvie, G. I. & Pringle, J. E. 2002, MNRAS, 337, 706

Muxlow, T. W. B., Pedlar, A., Holloway, A. J., Gallimore, J. F., & Antonucci, R. R. J. 1996, MNRAS, 278, 854

Natarajan, P., Armitage, P. J. 1999, ApJ, 506, L97

Nelson, R. P., Papaloizou, J. C. B. 2000, MNRAS, 315, 570

Ogilvie, G. I. 1999, MNRAS, 304, 557

Papaloizou, J. C. B., Lin, D. N. C. 1995, ApJ, 438, 841

Ray, T. P., Mundt, R., Dyson, J. E., Falle, S. A. E. G., Raga, A. C., 1996, ApJ, 468, L103

Sakimoto, P.J. & Coroniti, F., 1981, ApJ, 247, 19

Scheuer P. A. G., Feiler R. 1996, MNRAS, 282, 291

Shakura, N. I., Sunyaev, R. A. 1973, A&A, 24, 337

Wilkins, D. C. 1972, Phys. Rev. D, 5, 814

Wilson, A. S., & Ulvestad, J. S. 1987, ApJ, 319, 105

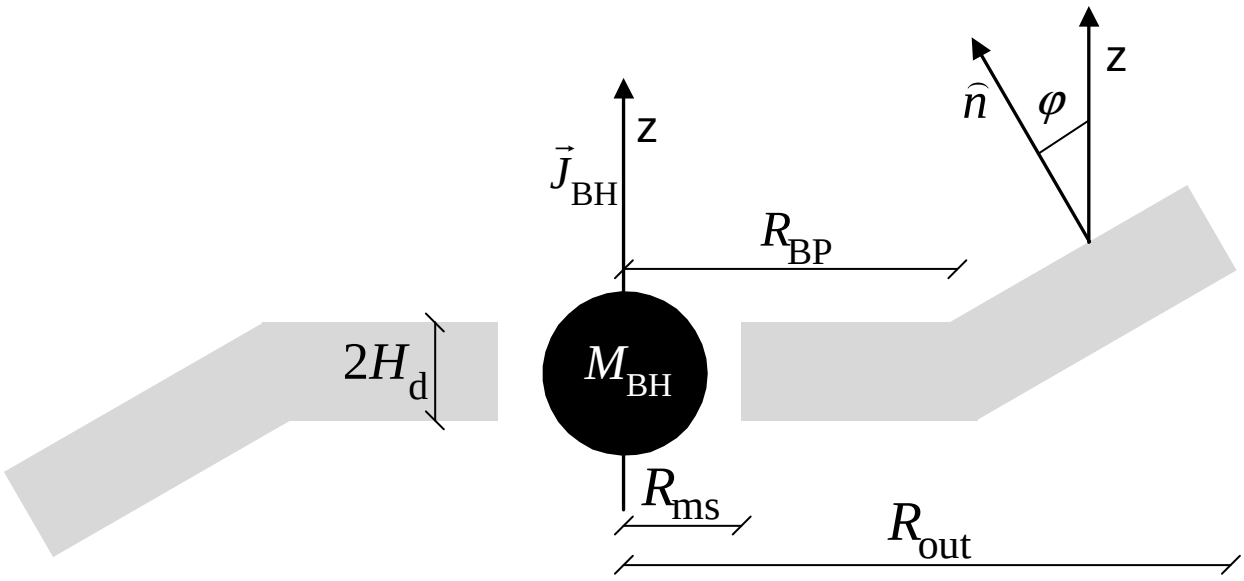

Fig. 1.— Schematic view of the Bardeen-Petterson effect. An accretion disk with inner and outer radius $R_{\rm ms}$ and $R_{\rm out}$ respectively, having a semi-thickness $H_{\rm d}$ and misaligned initially by an angle φ in relation to the angular momentum of the black hole $J_{\rm BH}$ and mass $M_{\rm BH}$, will be warped by the Bardeen-Petterson effect. The Bardeen-Petterson radius $R_{\rm BP}$ marks the transition between the aligned and misaligned disk in relation to the black hole's equator.

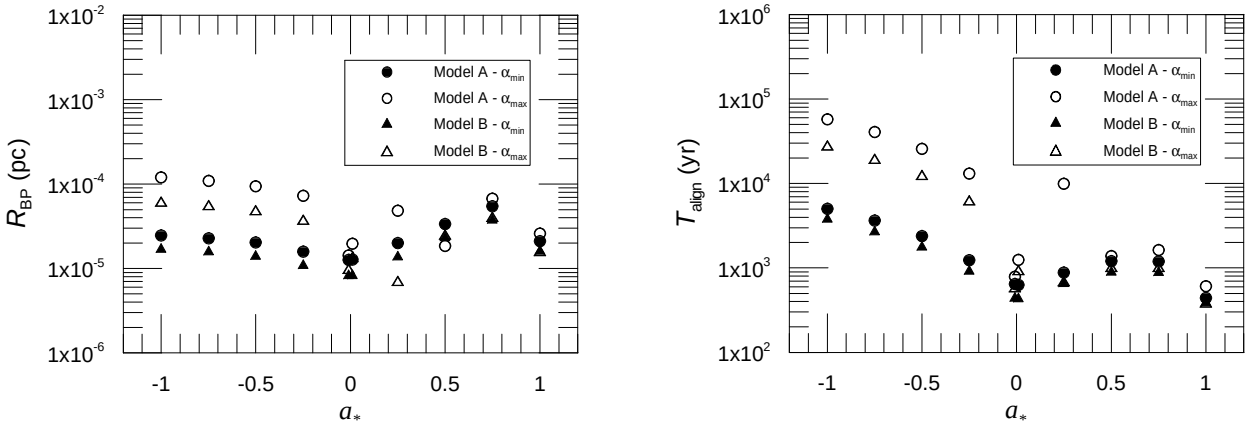

Fig. 2.— *Left panel*: Bardeen-Petterson radius as a function of the black hole spin for NGC 1068. Each point corresponds to the mean value of $R_{\rm BP}$ considering the limits of minimum and maximum accretion rate. Circles and triangles refer respectively to the models A and B. Filled symbols are related to the lower value of α-parameter, while open ones to its upper value. *Right panel*: Time-scale for alignment between accretion disk and the black hole's equator, using the same nomenclature for the symbols.

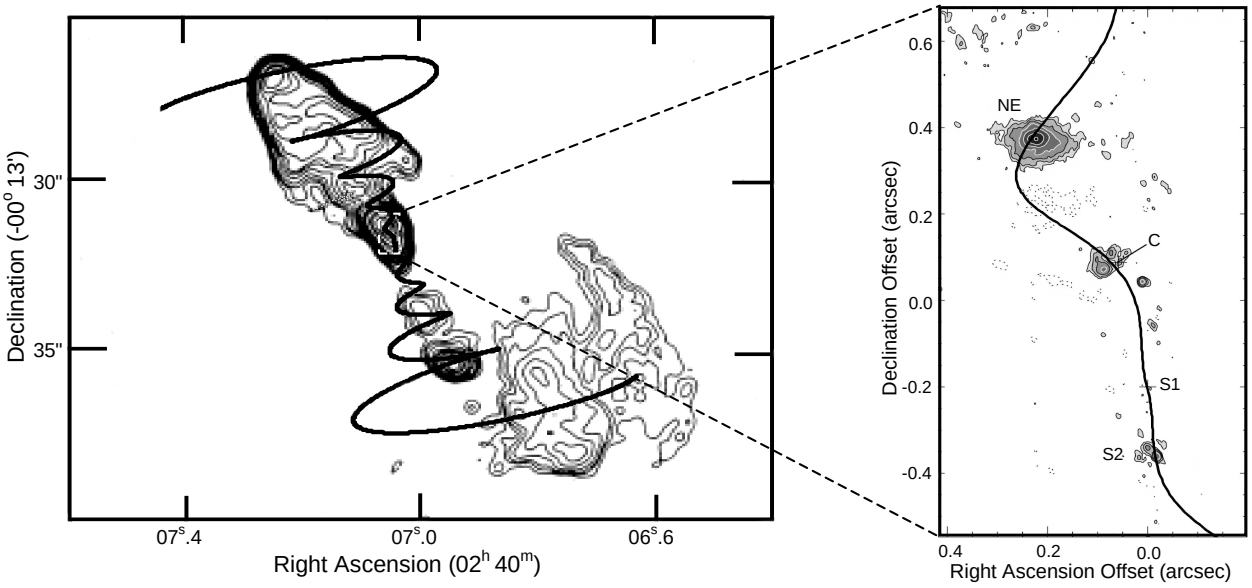

Fig. 3.— Snapshot of the changes in the jet orientation due to the Bardeen-Petterson effect. *Left panel*: Kiloparsec scale jet of NGC 1068 at 5 GHz (Wilson & Ulvestad 1987). Solid line indicates the model prediction from equations (9) and (10), assuming $\theta = 80°$, $v_{\rm jet} = 0.17c$, $t_0 = -9800$ yr, $T_{\rm align} = 7580$ yr, $\varphi_0 = 40°$ and $\eta = 17°$. *Right panel*: Comparison between the map at 1.4 GHz (Gallimore et al. 2004) with the same model shown in the left panel.

Table 1. Physical parameters of the disk.

Parameter	Model A	Model B
$M_{\rm BH}$ ($M_\odot$)	$(1.2 \pm 0.1)\times10^7$	$(8.0 \pm 0.3)\times10^6$
s	-1.05 ± 0.10	-1.05 ± 0.10
$M_{\rm d}$(r=1pc) ($M_\odot$)	$(9.4 \pm 1.6)\times10^6$	$(8.6 \pm 0.6)\times10^6$
Σ_0 (g cm^{-2})	$(1.06 \pm 0.23)\times10^9$	$(1.49 \pm 0.18)\times10^9$
$L_{\rm Edd}$ (erg s^{-1})	$(1.5 \pm 0.1)\times10^{45}$	$(1.0 \pm 0.3)\times10^{45}$
$\dot{M}/\dot{M}_{\rm Edd}$	0.46 - 1.0	0.71 - 1.0
$\alpha\epsilon(a_*)$	$(4.4$ - $9.4)\times10^{-4}$	$(4.4$ - $6.3)\times10^{-4}$

Note. — The quoted errors in $M_{\rm BH}$ and s are given by Huré (2002) and Lodato & Bertin (2003), while for Σ_0 were obtained from error propagation.